JOURNAL OF IMAGING SCIENCE AND TECHNOLOGY® • Volume 49, Number 4, July/August 2005

# Estimating the Absolute Quantum Yield of Sensitization for IR-Sensitive Photothermographic Imaging Materials

**Steven H. Kong**▲
*Eastman Kodak Company, Oakdale, Minnesota, USA*

One route to improving the photographic properties of PTG imaging materials and further the basic understanding of their photophysics is to better quantify the quantum yield of sensitization. A method was developed to estimate the absolute quantum yield of sensitization for IR-sensitive PTG imaging materials. The method utilizes three techniques: sensitometry, photobleach, and Monte Carlo simulation. Sensitometry and Monte Carlo simulation are well-known techniques. The photobleach technique is an optical technique developed to measure the absorptance of the dye adsorbed to the silver halide grains. The absorptance spectrum, by itself, is not sufficient because the absorption peak for dye adsorbed to silver halide and the absorption peak of dye not adsorbed to silver halide are not sufficiently shifted in position to allow us to resolve them. The photobleach technique is based on the discovery that the dye effectively adsorbed to the silver halide photobleaches much more readily. Using this distinction, the absorptance of the dye adsorbed effectively to the silver halide grains was extracted. The mean number of absorbed photons required to form a latent image was estimated to be 35 ± 7 for the PTG samples studied. In addition, practical applications of these techniques are discussed.

Journal of Imaging Science and Technology 49: 348–355 (2005)

## Introduction

The photothermographic (PTG) construction is a complex system that consists of the light capture element (silver halide grains), the silver source (silver carboxylate), and the development chemistry (developer, toners, and stabilizers) all integrated into one coating. Thus, the media can be processed dry with no additional chemistry. Due to this advantage over traditional silver halide film, PTG media have become widely used in laser imagers to generate hard copies for digital medical images. However, the complexity of this construction naturally makes troubleshooting or reformulation more difficult, especially in regards to film speed. If the film speed changes, it is difficult to determine if it is due to a change in chemical reactivity, a change in spectral sensitization, or a change in latent image formation efficiency. For instance, heat can destroy the IR dye, but it can also degrade the development chemistry. In order to help address this issue and also estimate the quantum sensitivity for infrared sensitive PTG media, a method for measuring the absolute quantum yield of sensitization for IR-sensitive PTG imaging materials was developed. While the measurement of the relative quantum yield of sensitization[1] is easier and more common, the results can be impacted by dye desensitization, and it does not provide an absolute measure of quantum sensitivity.

Ideally, we would like to quantify the quantum efficiency for each stage of the latent image formation process in a PTG material. While the efficiencies of various stages may be addressed, accurate estimates for all of them are beyond the scope of this article. The focus will be on estimating the number of absorbed photons per grain that are required to form a latent image. This threshold number of absorbed photons will be defined as $T_1$. The absolute quantum yield of sensitization will be defined as $1/T_1$. Another threshold of interest is the number of silver atoms required to form a latent image, $T_2$. $T_2$ will also be addressed, but an accurate estimate is not possible with the methods used.

The three techniques used in this method are sensitometry, photobleach and Monte Carlo simulation. From sensitometry, the photon flux incident on the film required to obtain a specific processed image density can be calculated. However, to determine the number of photons incident on the sensitizing dye adsorbed to silver halide, its absorptance needs to be measured. Making this measurement is difficult because only a small fraction of the sensitizing dye is adsorbed to silver halide in the samples studied. Furthermore, the absorption peak for dye adsorbed to silver halide and the absorption peak of dye not adsorbed to silver halide are not sufficiently shifted in position in order to resolve them. A photobleach technique was developed to make this measurement possible. With the absorptance of the dye adsorbed to silver halide, the $D$-Log $E$ curve can be transformed into a $D$-Log $Q$ curve, where $Q$ is the average number of photons incident on the adsorbed dye per grain. To extract the threshold for latent image

---

Original manuscript received December 24, 2004

▲ IS&T Member

Corresponding Author: Steven Kong, Steve.kong@kodak.com

**Table I. AgX Grain Coverage, Silver Coverage, AgR Coverage, and Sensitometric Parameters for the Three Main Samples for This Study**

| | AgXgrains/$\mu m^2$ | Agmol/$m^2$ | AgRmol/$m^2$ | Dmin | UDP | Speed |
|---|---|---|---|---|---|---|
| **Sample A** | 31 | 19.3 | 19.1 | 0.13 | 1.11 | 0.67 |
| **Sample B** | 124 | 19.6 | 18.7 | 0.17 | 2.95 | 1.43 |
| **Sample C** | 643 | 22.5 | 17.8 | 0.33 | 4.41 | 1.63 |

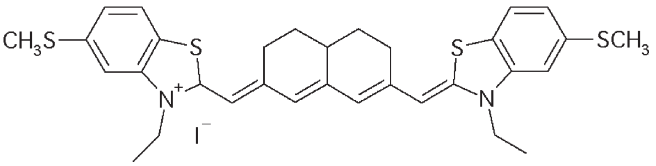

**Figure 1.** Chemical structure for Dye A.

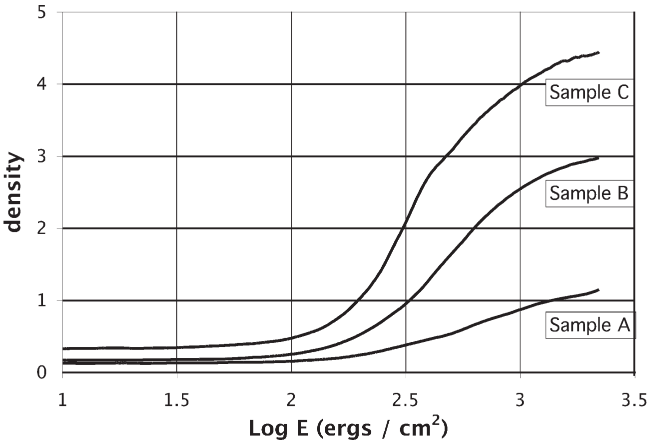

**Figure 2.** *D*-Log *E* curves for Sample A, Sample B, and Sample C.

formation, a Monte Carlo simulation was run to fit the D-Log Q curves. The threshold parameter values that gave the best fit were used to estimate the quantum yield of sensitization.

## Experiment

### *Photothermographic Construction*

The PTG construction used in the main study is the same as that studied in Ref. 2. It consists of small cubic grains and silver carboxylate (AgR) dispersed in a poly-vinyl butyral (PVB) binder along with a hindered phenol developer, toners, stabilizers, and antifoggants. The silver halide grains are chemically unsensitized, and they are spectrally sensitized in the near infrared with Dye A (Fig. 1).

Dye A is not added during the silver halide preparation process, but rather to the coating solution consisting of silver halide and silver carboxylate homogenized in MEK with a low concentration of PVB. However, antifoggants that generate in situ silver halide grains were avoided because these grains are difficult to characterize. Acutance dye was not used so that the light flux could be approximated as being the same throughout the photosensitive layer. Antihalation dye was retained on the backside coating in order to minimize back reflections, which simplifies the analysis.

The three main samples used in this study are listed in Table I. The upper density point (UDP) is defined as the density for Log *E* = 3.3. Speed is defined as 4 – Log *E* at the point where the density is 1.0 above *D*min. The exposure *E* is in units of ergs/cm$^2$.

The main difference between the three coatings is the silver halide coverage. All have a silver imaging layer thickness of about 20 µm, and the silver carboxylate coverage was targeted to be the same. The silver halide grains have an average equivalent circular diameter (ECD) of 72.2 nm. The width of the log normal distribution is about 0.07.

### *Sensitometry*

The film samples were given a continuous wedge exposure using a scanning 810 nm laser diode beam with a submicrosecond dwell time. The samples were processed thermally at 122°C for 15 seconds. The sensitometric strips were scanned using a custom built densitometer. The data collected are the visual density readings along the length of the continuous wedge from which the *D*-Log *E* curve is generated. A few sensitometric parameters are listed in Table I, and the sensitometric curves are displayed in Fig. 2.

### *Photobleach Technique*

In a PTG construction, a sensitizing dye molecule can be adsorbed to a silver halide grain, adsorbed to a silver carboxylate crystal, or unadsorbed. Absorbance spectroscopy studies seem to suggest that a fraction of the dye A molecules are adsorbed to the silver carboxylate crystals. In addition, we cannot rule out the presence of dye that is adsorbed to the silver halide grain, but which may be ineffective in transferring an electron on photoexcitation. The fraction of sensitizing dye molecules that are adsorbed to the silver halide grain and can effectively transfer a photoelectron will be referred to as "effective" dye molecules. The remaining dye molecules will be referred to as "ineffective" dye molecules. For the quantum sensitivity calculation, the absorptance of the effective dye molecules is required. A photobleach technique was developed to make this measurement. A preliminary photobleach experiment will be presented to provide a fundamental basis before the current implementation of this technique is described.

In the preliminary study, the total absorptance spectra were taken with a Perkin–Elmer Lambda-19 spectrophotometer that has a 6 inch integrating sphere. Samples were suspended in the middle of the sphere. Exposure to photobleach Dye A was made using an incandescent light bulb filtered with a Kodak Wratten gelatin filter 1A. A full photothermographic construction[3] with no acutance dye and no antihalation dye was prepared for this preliminary study. Unlike the samples used for the main study, this sample includes in situ silver halide grains.

The total absorptance spectrum of this construction has absorption contributions from both the effective and

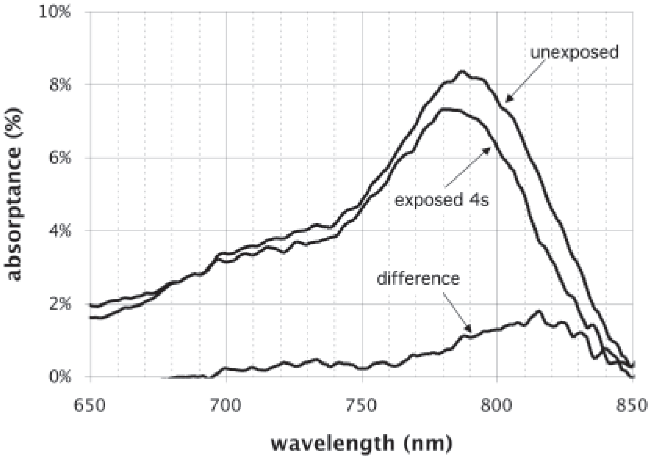

**Figure 3.** The total absorptance spectrum of a full photothermographic construction coated on 3 mil colorless PET with a silver coating weight of 2.4 g/m$^2$, before and after exposure, and the difference spectrum.

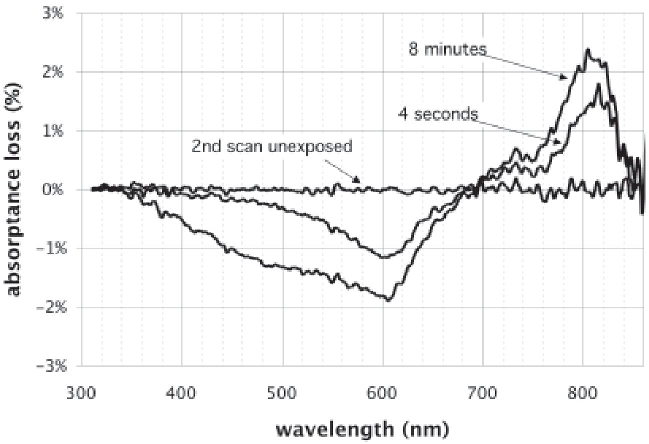

**Figure 4.** Difference spectra for exposures of 4 seconds and 8 minutes (sample as in Fig. 3). The base line spectrum was obtained by taking a second scan to determine if the exposure level of the spectrophotometer causes measurable bleaching.

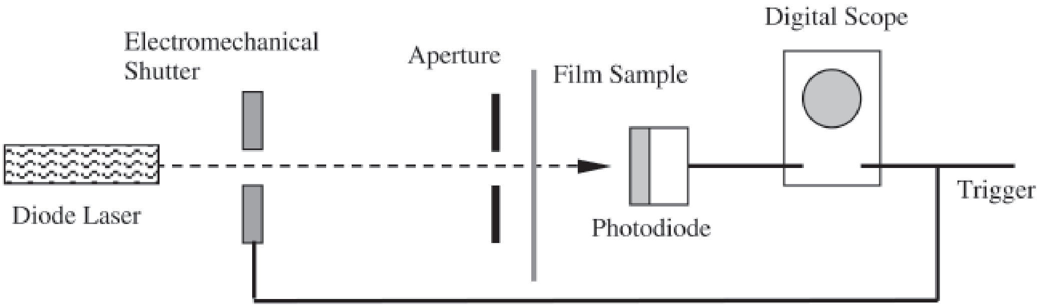

**Figure 5.** Photobleach set up. The trigger signal activates the shutter and oscilloscope.

ineffective dye (Fig. 3). To separate these contributions, the absorption spectrum is measured again after exposing the film to red light, which preferentially bleaches the effective dye. The difference between the unexposed and exposed spectrum of the film reveals the effective dye's absorption spectrum (Fig. 3), which peaks at about 810 nm. This is the wavelength where the sensitometric speed of the film peaks, which supports the conclusion that the dye bleached is "effectively" adsorbed. Note that after 4 seconds of photobleaching, the absorption peak position for the remaining unbleached dye has moved down to 785 nm. The peak position of dye not adsorbed to silver halide was determined to be at 785 nm by measuring the absorption spectrum for a coating with no silver halide. Therefore, after 4 seconds of exposure, essentially all of the effective dye has been bleached.

Prolonged red light exposure enhances the difference peak but shows a shift toward shorter wavelength (Fig. 4). At this point, the dye not adsorbed to silver halide is beginning to bleach. In addition, absorptance gain peaks are observed at 500 nm and 600 nm (Fig. 4). The peak at 600 nm is attributed to the radical dication of Dye A,[4] and the peak at 500 nm is attributed to printout silver. Therefore, in order for this photobleach technique to work, the sensitizing dye must have an absorptance peak sufficiently far from 500 nm and the region where the bleached dye absorbs. This restricts the usefulness of this technique to near-infrared and red absorbing dyes. Furthermore, this photobleach technique would not be practical for dyes that recover too quickly after being photobleached.

To simplify the photobleach technique, the measurement was made without an integrating sphere. The technique was further simplified by replacing the spectrometer with a transmission-measurement set up in which an 810 nm diode laser beam is transmitted through a film sample (Fig. 5). The transmitted beam intensity is monitored with a photodiode, and the resulting voltage levels are captured using a digital oscilloscope and a PC. The raw data collected are transformed into absorptance loss data by calculating the percentage change in the photodiode signal versus time and multiplying by a correction factor of 0.91 to take into account light scattering by Dye A. The relative amount of absorbed light was measured to be 91% for Dye A at 810 nm relative to the total amount of light absorbed or scattered. This technique has the advantage that the bleach time and measurement time are much shorter, which minimizes the number of bleached dye that recovers.

Representative photobleach traces from this technique are shown in Fig. 6. The initial exposure results in rapid photobleaching of Dye A in Sample C. The rate of photobleaching decreases with time and the trace begins to saturate. Since additional exposure will bleach the

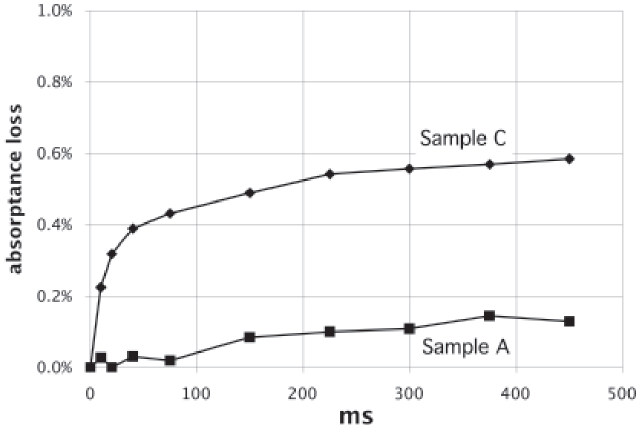

**Figure 6.** Photobleach traces. Each trace is an average of five measurements.

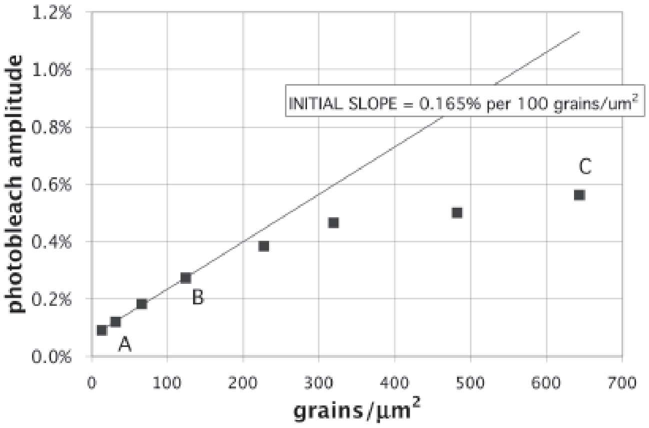

**Figure 7.** Photobleach amplitude versus silver halide grain number for Samples A, B, and C.

ineffective dye, the trace will not completely saturate. Therefore, a “saturation” region will be loosely defined as the region past the shoulder of the trace where the slope is not changing significantly. The absorptance loss data points in the front portion of the “saturation” region are averaged, giving a measurement that will be referred to as the photobleach amplitude. Essentially all of the effective dye molecules are bleached at this point. The slow linear rise in the saturation region is due to the photobleaching of the ineffective dye molecules. This conclusion is supported by the preliminary study and can be further verified by the photobleach trace for Sample A. Although Sample A has a factor of twenty fewer silver halide grains, the rate of photobleaching in the saturation region is the same as that for Sample C. Thus the bleaching in this region must be dominated by the bleaching of dye molecules that are not adsorbed to the silver halide grains. Any contribution by ineffective dye molecules adsorbed to the silver halide grains is minimal.

The contribution from dye not adsorbed to the silver halide grains can be determined by measuring the photobleach amplitude of a sample with no silver halide grains or extrapolating to zero the linear portion of a photobleach amplitude vs. silver halide concentration plot (Fig. 7). Once determined, this contribution can be subtracted out to give the absorptance for the effective dye molecules.

## Experimental Results

The photobleach amplitude was measured for several film samples with different concentrations of silver halide grains (Fig. 7). Samples A, B, and C were chosen from this set. The y-intercept of the photobleach amplitude vs grain number plot gives the photobleach contribution from the dye molecules not adsorbed to silver halide, which can be subtracted to give the absorptance of the effective dye molecules. The photobleach amplitude is less for these samples than the sample used in the preliminary study since the in situ halidization also promotes dye adsorption.

The results from the photobleach study are given in Table II. Since the amount of Dye A added was kept constant, the number of effective dye molecules per grain is less for sample C, which had the highest level of silver halide grains. The number of effective dye molecules per grain was calculated by using the effective dye absorptance, extinction coefficient of Dye A in methanol (220,000 $M^{-1}cm^{-1}$) and the grain number (Table I). It is understood that the extinction coefficient may differ when adsorbed to silver halide compared to solvent, so the number of effective dye molecules is a parameter that is varied in the modeling. Note that the number of effective dye molecules per grain is not used to determine Q but determines the frequency at which an effective dye molecule receives more than one incident photon.

**Table II. Absorptance and Number of Effective Dye A Molecules for the Three Main Samples of This Study**

| | Absorptance | | Number | |
|---|---|---|---|---|
| | % | Relative | #/grain | Relative |
| Sample A | 0.051 | 0.25 | 215 | 1.00 |
| Sample B | 0.204 | 1.00 | 215 | 1.00 |
| Sample C | 0.492 | 2.41 | 100 | 0.47 |

Using the slope from Fig. 7, the $D$-Log $E$ curves can now be transformed into $D$-Log $Q$ curves, where $Q$ is the average number per grain of photons incident on effective dye. $Q$ is equal to the quantum exposure (photons/$cm^2$) times the absorptance of the effective dye divided by the number of grains/$cm^2$. If the effective dye molecules do not photobleach, $Q$ is simply the average number of absorbed photons per grain.

In calculating Log $Q$ from Log $E$, a correction factor was used to account for reflection at the interfaces and absorption by the silver layer. This was necessary since Log $E$ represents the amount of light from the laser and not the amount of light incident on the silver halide grains. Reflectance calculations based on the refractive indices of the base and silver layer and the silver layer absorbance at 810 nm gave a correction factor of –0.02 for Log E.

## Analysis

### *Monte Carlo Simulation*

It is not clear at which point on the $D$-Log $Q$ curves correspond to the threshold for latent image formation. If the grains have a wide distribution for the threshold, the inertial speed point may be close to the minimum threshold point.[5] The inertial speed point is defined as the point on the Log $E$ axis where a line extrapolated from the linear portion of the $D$-Log $E$ curve crosses the $D$min point. If the threshold were sharp, the threshold would be near

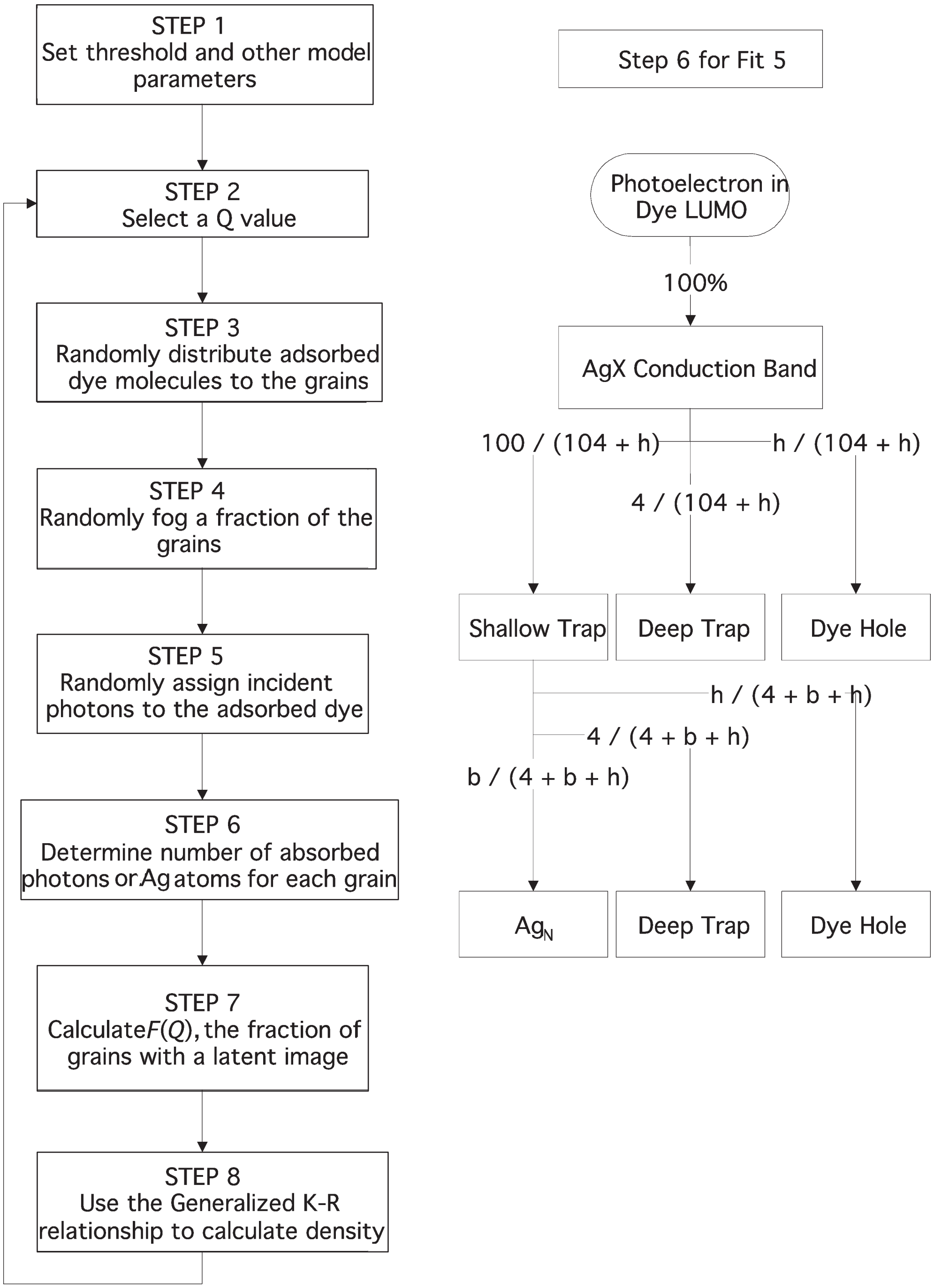

**Figure 8.** Left: The main steps in the Monte Carlo simulation. Right: Details of Step 6 for Fit 5. The label on a branch is the probabilities assigned to that path. These steps are iterated for each photoelectron that is generated on a grain. If $N < 3$, $b = 3$ (nucleation); if $N > 2$, $b = 60$ (latent image growth). The number of dye holes, $h$, and $N$ are initialized to zero for each grain.

the point where half of the grains have a latent image. However, the spread in grain size may shift the threshold point away from this halfway point. To make a more precise estimate, Monte Carlo simulations of 20,000 grains were run to fit the $D$-Log $Q$ curves. The Poisson statistical approach of Dainty and Shaw[5] should give the same results, but the Monte Carlo approach was chosen since it is easier to adapt for more complex cases.

The steps in the simulation are summarized in Fig. 8. First, the threshold level and other parameters are selected (Table III). The values for most of the parameter estimates are from experimental data. Both the grain size and the threshold are assumed to have a log normal distribution, and the mode for each distribution is listed. The grain size is given in terms of equivalent circular diameter (ECD). Log (ECD) σ is the standard deviation of the log grain size distribution, and Log ($T$) $\sigma$ is the standard deviation of the Log $T_1$ or Log $T_2$ distribution. *NDye* is the average number of effective dye molecules per grain.

$D_o$ and $n\upsilon$ are parameters from the generalized Klosterboer–Rutledge (K–R) relationship (Eq. (1)).[2] This relationship is used to calculate the density $D$ for a given $F$, the fraction of silver halide grains that have a latent image. The reactivity parameter $n\upsilon$ is the grain number density (#/μm$^3$) times the sphere of influence volume (μm$^3$). $D_o$ represents the density achieved when all of the AgR is developed.

$$D = D_o\left(1 - \exp[-n\upsilon F]\right) \tag{1}$$

Equation (1) assumes that the covering power of the image silver is constant. Ito, et al.[6] have proposed a model that attempts to account for a covering power that changes with latent image number density. However, this relationship gave a poorer fit to the data in this study, so Eq. (1) was selected. Furthermore, Ohzeki has shown that a solvent-based photothermographic construction shows little variation in covering power with exposure.[7]

After the parameters are initialized and a value for $Q$ selected, the effective Dye A molecules are randomly assigned to the grains in a manner to give a constant number of dye-per-unit surface area. A fraction of the silver halide grains are randomly fogged to achieve the observed Dmin. The number of photons incident on the effective dye molecules is calculated using the absorptance values in Table II. In Fit 4, where the absorption cross section for Dye A was assumed to be symmetric, the incident photons were randomly assigned to the effective dye molecules with equal weighting. In the other fits, where the absorption cross section for dye A was assumed to be anisotropic, the dye molecules were randomly oriented. The cross section was assumed to be proportional to $\cos^2\theta$, where $\theta$ is the angle between the dye axis and the optical electric field.[8] The random assignment of photons to the dye molecules was weighted with these cross sections.

In Step 6, the number of absorbed photons for each grain is counted for Fits 1 through 4, and the number of $Ag^0$ atoms is counted for Fit 5. Fits 1 through 4 assume that each effective dye molecule can only absorb one photon. If an effective dye molecule has more than one incident photon assigned to it, only one is absorbed. However, this ignores the possibility of the recombination of an injected electron with a dye hole, which would allow the possibility for a second photon to be absorbed. To address this fully would require a comprehensive Monte Carlo simulation for the trapping, latent image formation, and recombination stages,[9] which is beyond the scope of this article. Nevertheless, Step 6 was enhanced for Fit 5 in an attempt to provide a crude simulation of these stages (Fig. 8).

In Step 8, the $F(Q)$ calculated in Step 7 is plugged into Eq. (1) to obtain $D(Q)$. Steps 2 to 8 are repeated until the full $D$-Log $Q$ curve is generated. The simulation is run repeatedly to find parameters that gave the optimal fit to the $D$-Log $Q$ curves. The parameters were allowed to vary near the initial estimates and significant departures from these initial estimates were only used as a last resort.

An error analysis for $T_1$ was carried out by varying $T_1$ until a good fit was not achievable for reasonable parameter values. This resulted in an error estimate of ± 15%. Since rigorous error data were not available for the initial parameter, this is only a rough estimate. Taking into account errors introduced by sensitometry and the photobleach method, an overall error estimate of ± 20% was inferred.

### *Threshold for Latent Image Formation*

Five fits were obtained using the Monte Carlo simulation (Table III), the first three of which are plotted in Fig. 9. The results for the additional parameters required for Fit 5 are shown in Fig. 8. Note that the electron transfer efficiency was taken to be 100% for all of the fits since it does not impact $T_1$ directly, only $T_2$.

All five cases gave reasonably good fits for the $D$-Log $Q$ curves. The most difficult curve to fit was for Sample 3. In each case, one parameter was adjusted significantly away from its initial estimate in order to obtain a good fit for this sample. Most of the fits have significantly lower $n\upsilon$ values for Sample C. It is likely that at much higher grain number densities, grain clumping has occurred, which is a problem with small silver halide grains.[10] However, Fit 2 has reasonable $n\upsilon$ values for Sample C, but has a lower number of effective dye molecules per grain. Therefore, having fewer effective dye molecules per grain can also account for this discrepancy. In either case, Fit 1 and Fit 2 gave very similar thresholds.

Fit 5 was included in attempt to determine if accounting for electron traps and dye holes can possibly resolve the difficulty of fitting the data for Sample C. Since the relative trapping cross sections and recombination cross section were chosen blindly, the results are only good for this purpose. By varying these cross sections, a better fit was not found. Fit 5 is a representative fit and resulted in a $T_2$ of 17. This was not included in Table III since it is not a true estimate.

Varying the average amount of effective dye molecules per grain from 100 to infinity changes the threshold by less than 20%, while the fit for the D-Log Q curve degrades. Therefore, the final results are not overly sensitive to the amount of dye per grain. It must be kept in mind that the amount of dye per grain is not used to calculate the number of absorbed photons per grain, but rather to make sure a single dye does not absorb two or more photons.

Fit 1 was selected as the best fit. The threshold distribution for Fit 1 has a mode of 32 ± 6 and a mean of 35 ± 7. The Log $T_1$ distribution width equals 0.25, so 95% of the threshold levels lie between 10 and 100. The inertial speed points for the three samples are between $Q = 10$ and $Q = 14$. Thus, the inertial speed point provides a reasonable estimate for the minimum threshold for this particular fit. Since it is conceivable for the width of the grain size distribution to increase after they have been incorporated into the silver carboxylate homogenate, the true range of threshold levels may have a significant uncertainty. While the width of the grain size distribution used in the model directly impacts the width of the threshold distribution, it does not directly impact the mean threshold.

The silver halide grains in this study have no chemical sensitization; therefore, the quantum yield is reasonably good and not far from typical wet silver halide emulsions, which usually requires 10 to 30 absorbed photons to create a latent image. It is clear from this study that most of the speed opportunities lie in improving the light capture efficiency. The particular construction studied has fewer effective dye molecules than typical as a result of the omission of in situ halidization. Nevertheless, even the full construction utilizes less than 3% of the incident light.

## Application

While all three techniques are required to estimate the absolute quantum yield, the photobleach technique and

**TABLE III. Initial Estimates and Resulting Fits for the Monte Carlo Simulation Parameters**

| Parameters | Estimates | Fit 1 | Fit 2 | Fit 3 | Fit 4 | Fit 5 |
|---|---|---|---|---|---|---|
| mode of ECD (nm) | 71 | 71 | 71 | 71 | 71 | 71 |
| Log (ECD) $\sigma$ | 0.070 | 0.070 | 0.070 | 0.070 | 0.070 | 0.070 |
| $n\upsilon$ (B) | 0.09 | 0.94 | 1.05 | 0.9 | 0.85 | 0.93 |
| $n\upsilon$ (A)/$n\upsilon$ (B) | 0.25 | 0.25 | 0.25 | 0.25 | 0.25 | 0.25 |
| $n\upsilon$ (C)/$n\upsilon$ (B) | 5.20 | 3.5 | 4.55 | 2.70 | 3.00 | 3.53 |
| $D_o$ (B) | 4.50 | 4.87 | 5.00 | 4.96 | 5.07 | 5.12 |
| $D_o$ (A)/ $D_o$ (B) | 1.02 | 1.00 | 1.02 | 1.00 | 1.02 | 1.02 |
| $D_o$ (C)/ $D_o$ (B) | 0.95 | 0.97 | 0.98 | 0.96 | 0.95 | 0.93 |
| Dye Symmetry | asymmetric | asymmetric | asymmetric | asymmetric | symmetric | asymmetric |
| *Ndye* (B), avg #/grain | 215 | 215 | 100 | infinite | 215 | 215 |
| *Ndye* (A)/*Ndye* (B) | 1 | 1 | 1 | 1 | 1 | 1 |
| *Ndye* (C)/*Ndye* (B) | 0.47 | 0.4 | 0.4 | 1 | 0.4 | 0.4 |
| Percent fogged | – | 1.3% | 1.3% | 1.7% | 1.7% | 1.5% |
| **Log ($T$) $\sigma$** | – | **0.25** | 0.25 | 0.3 | 0.25 | 0.22 |
| **mode of $T_1$** | – | **32** | 31 | 37 | 32 | – |
| **mode of $T_2$** | – | – | – | – | – | see text |

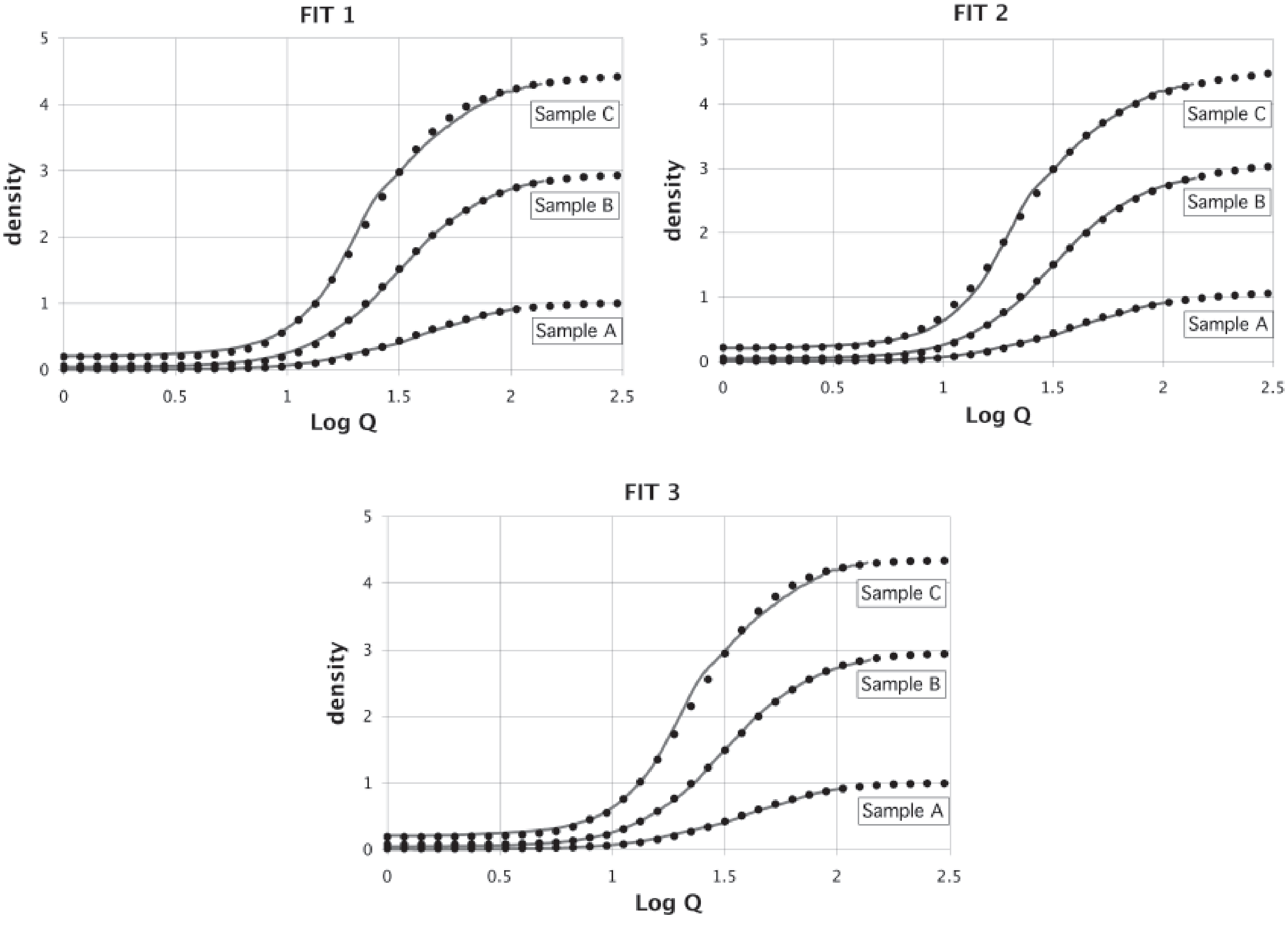

**Figure 9.** Experimental $D$-Log $Q$ curves (solid line) and $D$-Log $Q$ curves from the Monte Carlo simulations (solid circles).

sensitometry can be used together to determine if a speed change is due to a change in the amount of effective sensitizing dye. A factor of two change in the amount of effective dye should result in a one-stop change in speed, assuming there are no significant desensitization effects. To facilitate this analysis, a photobleach speed is defined as

$$\text{Photobleach Speed} = \text{Sensitometric Speed (reference)} + \log (A_1/A_0), \qquad (2)$$

where $A_0$ is the photobleach amplitude of a reference sample, and $A_1$ is the photobleach amplitude of the test sample. If the change in photobleach speed is equal to the change in sensitometric speed, the change in speed is most likely due to a change in the amount of effective dye.

A simple case where this statement can be tested is for a dye level series, since the amount of effective dye is the only variable expected to change. In Fig. 10, the photobleach speed is compared with the sensitometric speed for a typical PTG construction with different Dye A levels. The inertial speed was used in this comparison. The photobleach speed closely tracks the sensitometric speed, thus verifying the statement above. In addition, Eq. (2) was used to calculate a speed using the 810 nm absorptance in place of the photobleach amplitude. The speeds calculated from the 810 nm absorptance do not track the sensitometric speed well at higher dye levels, showing that increasing the dye concentration did not proportionally increase the amount of effective dye. The utility of this approach can clearly be seen.

Other speed points, such as the one at Dmin + 1.0, did not compare as well to the photobleach speed because the UDP is lower for the lowest dye level. The problem is that this speed point will shift in position on the sensitometric curve from below the inflection point to above the inflection and up onto the shoulder as the UDP decreases. Ideally, what should be used is a speed point that does not change its relative position on the sensitometric curve as the UDP changes, such as the inertial speed. However, in a case where UDP does not change significantly, these other speed points would be suitable and possibly more desirable because they are more meaningful metrics for a product.

## Summary

A method was developed to estimate the absolute quantum yield of sensitization for IR-sensitive PTG imaging materials. The method utilizes three techniques: sensitometry, photobleach, and Monte Carlo simulation. From sensitometry, the incident photon flux required to obtain a specific processed image density was calculated. A photobleach technique was developed to measure the absorptance of the effective dye molecules from which the photon flux incident on the effective dye was calculated. Using this, the $D$-Log $E$ curve was transformed into a $D$-Log $Q$ curve, where $Q$ is the average number of photons incident on the effective dye molecules per grain. The threshold for latent image formation was estimated by using a Monte Carlo simulation to fit the $D$-Log $Q$ curves for three samples with different silver halide levels. The estimated, mean number of absorbed photons required to form a latent image is 35 ± 7 for the PTG samples studied, which corresponds to quantum yields between 1/28 and 1/42. Therefore, this method can be used to estimate the quantum yield for PTG constructions that incorporate a sensitizing dye that photobleaches, typically near-infrared dyes and some red dyes. By limiting the techniques to sensitometry and photobleach, this method can be greatly simplified. The simplified method can be used to determine if a speed degradation or enhancement is caused by the change in the amount of effective dye with much less effort than implementing the full study outlined in this article.

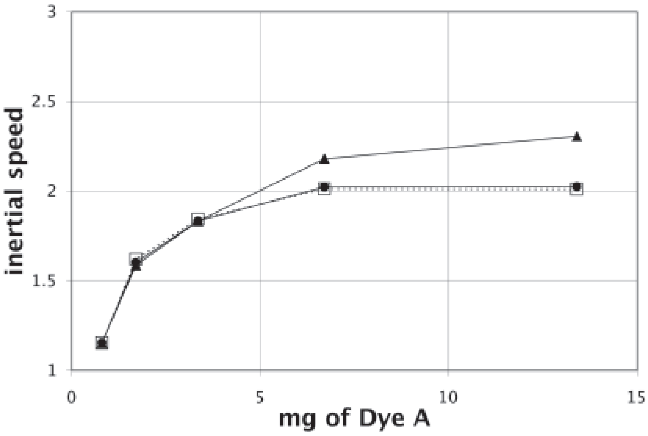

**Figure 10.** Comparison of sensitometric speed (filled circles) with speed calculated from the photobleach amplitude (open squares) and the 810 nm Dye A absorptance (solid triangles) for different levels of Dye A in a typical PTG construction. The lowest level for Dye A was chosen as the reference level for Eq. (2).

## References

1. W. West and P. B. Gilman, in *The Theory of the Photographic Process,* 4th ed, T. H. James, Ed. (Macmillian, New York, NY, 1977), p. 255.
2. S. H. Kong, *J. Imaging Sci. Technol.* ISSN: 1062-3701, **43**, 509 (1999).
3. C. Zou, J. B. Phillip, S. M. Shor, M. C. Skinner, and P. Zhou, US Patent 5,434,043 (1995).
4. J. R. Lenhard, B. R. Hein and A. A. Muenter, *J. Phys. Chem.* **97** (1993), p. 8269.
5. J. C. Dainty and R. Shaw, *Image Science*, (Academic Press, NY, 1974), chap. 3.
6. T. Ito, S. Nishiwaki and T. Mitsuhasi, *J. Imaging Sci. Technol.* ISSN: 1062-3701, **45**, 357 (2001)
7. T. Ohzeki, *IS&T/SPSTJ 2004 International Symposium on Silver Halide Technology*, (IS&T, Springfield, VA, 2004), p. ???.
8. I. P. Kaminow, L. W. Stulz, E. A. Chandross, and C. A. Pryde, *Appl. Opt.* **11**, 1563 (1972).
9. B. E. Bayer and J. F. Hamilton, *J. Opt. Soc. Amer.* **55**, 439 (1965).
10. E. Fuchs, *Photogr. Ind.* **28**, 1172 (1930).